

# Astrophysics and Dark Matter Theory

Auguste Meessen

UCL, Louvain-la-Neuve, Belgium

Email: [auguste@meessen.net](mailto:auguste@meessen.net)

**How to cite this paper:** Meessen, A. (2017)  
Astrophysics and Dark Matter Theory.  
*Journal of Modern Physics*, 8, 268-298.  
<https://doi.org/10.4236/jmp.2017.82018>

**Received:** December 17, 2016

**Accepted:** February 25, 2017

**Published:** February 28, 2017

Copyright © 2017 by author and  
Scientific Research Publishing Inc.  
This work is licensed under the Creative  
Commons Attribution International  
License (CC BY 4.0).  
<http://creativecommons.org/licenses/by/4.0/>



Open Access

---

## Abstract

Space-Time Quantization implies that the cosmic dark matter gas is subjected to pressure effects. We prove this by accounting for the mass-density distribution of dark matter in galactic halos. It can be directly deduced from observed rotation curves and coincides with theoretical predictions for dark matter atmospheres in hydrostatic equilibrium. Through embedding, the pressure of the cosmic dark matter gas prevents also the gravitational collapse of the Oort cloud, globular star clusters and cosmic filaments. The Sun has only a very small dark matter atmosphere, but observations confirm that dark matter is orbiting around the Sun. Other facts are explained by planetary dark matter disks. Space-Time quantization accounts also for dark matter-electron interaction, which allowed already for direct detection of galactic dark matter particles.

## Keywords

Dark Matter, Space-Time Quantization, Dark Matter Density Distribution, Dark Matter Rings, Pioneer Anomaly, Flyby Anomaly

---

## 1. Introduction

The idea that our universe could contain “dark matter” was unexpected. It was formulated by *Zwicky* in 1933, since his measurements of the velocities of nebula in the Coma cluster revealed a very high average value and a great dispersion. He analyzed this data by means of the virial theorem of statistical mechanics, which applies to any spherical distribution of equal masses, subjected to gravitational interactions. He stated [1] that “if these optical observations were confirmed, they would yield the surprising result that dark matter (*dunkle Materie*) is present at much greater densities than luminous matter.”

This seemed to be unbelievable, but the breakthrough came in the 1970s, because of the tenacity of *Vera Rubin*. She measured the redshift of many stars in the Andromeda galaxy [2] [3] [4]. The resulting dependence of orbital velocities

on the distance to the galactic center required the existence of Dark Matter (DM). It had even to be present far beyond the visible boundaries of galaxies. *Albert Bosma* confirmed this conclusion by means of the 21-cm hydrogen line [5] [6]. He determined the mass  $M$ , which causes the observed orbital velocities by gravity. He measured also the optically detectable light intensity  $L$  and concluded that “there is a large amount of high  $M/L$  material in the outer parts.” There is not only more mass than the visible one, but it “may not be distributed in the disk at all”. Actually, it constitutes a very great spherical halo.

Nevertheless, the existence of DM in our universe is still subject to controversies. The main reason is that DM particles have not yet been identified and that measured rotation curves can also be fitted by assuming a modification of Newton’s law of gravity [7]. A recent analysis of excellent empirical data for 153 galaxies of different morphologies, masses, sizes and gas content led even to a very puzzling result [8]. The *observed* gravitational acceleration, determined by means of the rotation curves, was always correlated in a simple way with the *baryonic* acceleration, calculated by means of the distribution of luminous matter. This can suggest that DM may not be needed [9] and requires an explanation. There are also other ambiguities that have to be clarified.

Could the theory of Space-Time Quantization (STQ) be helpful in this regard? It generalizes Relativistic Quantum Mechanics by considering a finite limit for the smallest measurable distance. It is sufficient that its value  $a \neq 0$ , to prove that STQ accounts for elementary particle physics [10]. It yields also insight into the nature and properties of DM particles. This solves basic cosmological problems [11], but we want also to test the proposed theory by means of a variety of astrophysical observations. This is the essential aim of the present article.

It may thus be useful to recall some basic consequences of the proposed theory. All elementary particles are characterized by four new quantum numbers  $(u_x, u_y, u_z, u_{ct})$ . They specify possible variations of  $\psi$  functions at the smallest possible scale along the chosen reference axes. These  $u$ -quantum numbers are subjected to a very strict conservation law when particles are transformed by annihilation and creation processes. This law determines all possible types of interactions and the constitution of compound particles [10]. We can thus distinguish three levels. 1) The basic level concerns only elementary particles. There are *quarks*, but also elementary DM particles, which interact with one another by exchanging gluons. Since they are electrically neutral, we called them *narks*. 2) On the second level, quarks get bound to one another inside *nucleons*, while narks can constitute various types of *neutralons*. Nucleons interact with one another by exchanging  $\pi$  mesons and neutralons by exchanging  $N_2$  bosons, composed of a nark and an antinark. This allows in both cases for scattering and the formation of compound particles. 3) The third level concerns the resulting particles. Baryonic matter is constituted of single nucleons or nuclei, where nucleons are bound together. The cosmic DM gas contains neutralons and compound DM particles, where neutralons are bound to one another.

DM particles of any type do not interact with baryonic matter [10], but they

are subjected to gravitational interactions, because of their mass. Moreover, compound DM particles allow for fusion and fission processes everywhere in the cosmic DM gas. This accounts for “dark energy” and is important for cosmology [11]. However, DM particles are usually only scattered by one another. Because of energy quantization, elastic scattering is predominant. DM particles behave thus like molecules in ordinary gasses and the cosmic DM gas has some pressure. This concept will be essential for this article.

It is organized in the following way. In chapter 2, we show that the density distribution of DM inside spherically symmetric *galactic halos* can be directly deduced from rotation curves. This empirical result is then explained by combining gravity with pressure effects. We discuss also related problems, especially for the Solar system. In chapter 3, we consider cases where gravitational collapse of ordinary matter is prevented, since it is *imbedded* in the cosmic DM gas. This mechanism is especially important for the gigantic cosmic filaments, where galaxies remain separated, although they attract one another. Chapter 4 is devoted to the study of *DM rings*. Chapter 5 completes the previous discussion [10] of detection or production of DM particles. Instead of DM-nucleon interactions, we consider now *DM-electron interactions*. They explain why galactic DM particles could already be detected by means of scintillators.

## 2. Spherically Symmetric Dark Matter Atmospheres

### 2.1. Empirical DM Density Distribution in Galactic Halos

To determine the radial distribution  $\rho(r)$  of the DM mass density in spiral galaxies, we adopt the model of **Figure 1**. There are many visible stars and baryonic particles in the galactic disk, but we consider only one of them. The orbital velocity  $v$  of this “test body” can be determined by measuring the Doppler shift of its radiation. Assuming a circular orbit of radius  $r$ , this implies a radial

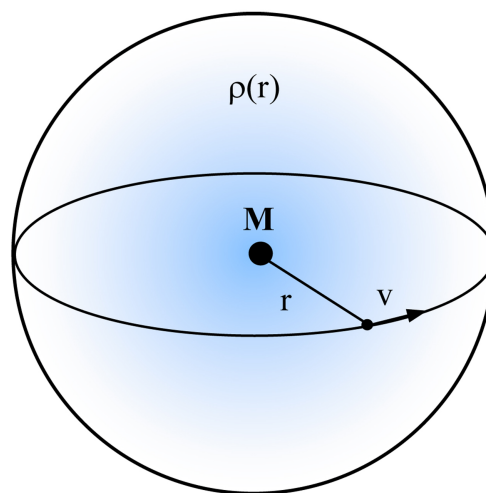


**Figure 1.** The DM atmosphere in the sphere that has the same radius  $r$  as an orbit in the galactic disk.

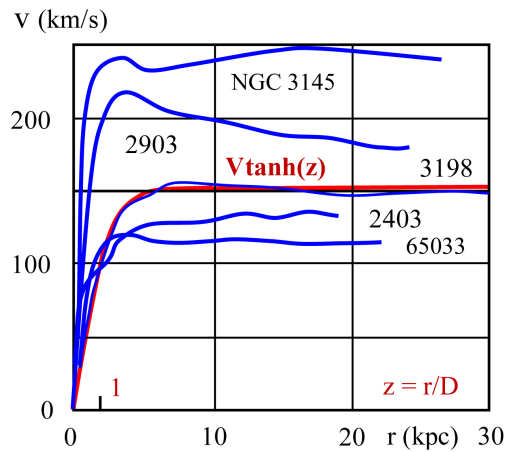


**Figure 2.** Observed rotation curves (in blue) and proposed model function (in red).

acceleration  $g = v^2/r$ . It is due to gravitational attraction towards the center of the galaxy, but we can consider that all masses in the galactic disk are negligible with respect to the mass  $M$  of the central supermassive black hole. It follows then from Newton’s law of gravity that  $g = GM/r^2$ . This would yield Kepler’s law  $v^2 = GM/r$ , but the observed rotation curves  $v(r)$  are totally different (**Figure 2**). When  $r \rightarrow 0$ , we get a linear variation:  $v(r) = \omega r$ , while  $v(r)$  tends towards a constant value  $V$  when  $r \rightarrow \infty$ . Galactic rotation curves are said to be “flat”. Sometimes the linear increase of  $v(r)$  near the center of the galaxy is followed by a “bump” and the spiral arms can lead to oscillations of  $v(r)$ . Some rotation curves display only the rising part [7], but this can be interpreted as resulting from a low value of  $\omega$  for these galaxies. We propose therefore that all observed rotation curves are (in first approximation) of the same type as the red one in **Figure 2**. It represents *empirical* results by means of the simple universal function:

$$v(r) = V \tanh(r/D) \quad \text{or} \quad y(z) = \tanh(z) \quad (1)$$

There are only two parameters:  $V$  and  $r$ , while  $y = v/V$  and  $z = r/D$ . The intermediate curvature is adequate and the distance  $D$  corresponds to the value of  $r$  where the extrapolated straight line  $v(r) = \omega r$  meets the horizontal line  $v(r) = V$ . The parameters  $D$  and  $V$  define natural units for the horizontal and vertical axes in **Figure 2**. Different galaxies are characterized by particular values of  $D$  and  $V$ .

Relation (1) summarizes empirical data in a unified and flexible way, by separating essential features from secondary ones. We can express this result in another way, since the rotation curve  $v(r)$  is determined by the condition of dynamical equilibrium. The orbiting test body is attracted towards the center of the galaxy, but not only by the mass  $M$  of the central black hole. It is also necessary to take into account the total mass  $Mr$  of the spherically symmetric distributed DM up to the radius  $r$  (**Figure 1**). The term “halo” does simply result from an analogy with light of decreasing intensity for greater and greater distances.

Actually, we should consider the radial *mass-density distribution*  $\rho(r)$  of DM. This function is related to the measured rotation curves, since the radial acceleration is

$$g(r) = \frac{G}{r^2}(M + Mr) = \frac{v^2}{r} \quad \text{where} \quad Mr = 4\pi \int_0^r \rho(r) r^2 dr \quad (2)$$

We expect that the mass-density  $\rho(r)$  reaches its highest value  $\rho_o$  at the center of the galaxy and that it is there nearly constant. It follows that

$$\begin{aligned} GM + \frac{4\pi G \rho_o}{3} r^3 \\ = rv^2 = \left(\frac{V}{D}\right)^2 r^3 \quad \text{for } r \rightarrow 0 \end{aligned}$$

Since the mass  $M$  is independent of  $r$ , the density  $\rho_o$  is so enormous that  $Mr \gg M$ , even for small values of  $r$ . Moreover, it is possible to deduce the central mass density  $\rho_o$  from the measured values of  $D$  and  $V$ , but it will be more useful to define  $D$  in terms of  $\rho_o$  and  $V$ . We can thus express  $\rho(r)$  in natural units, so that:

$$\rho(r) = \rho_o f(z) \quad \text{where} \quad z = \frac{r}{D} \quad \text{and} \quad D^2 = \frac{3V^2}{4\pi G \rho_o} \quad (3)$$

Because of (2), we get then an integral equation:

$$3 \int_0^z f(z) z^2 dz = zy^2 \quad \text{or} \quad f(z) = \frac{y^2 + 2zyy'}{3z^2} \quad (4)$$

The shape of the galactic DM density profile  $\rho(r)$  can thus be directly deduced from the observed rotations curves  $v(r)$ . The function  $f(z)$  follows from  $y(z)$  and vice-versa. When  $z \rightarrow 0$ , we get  $y(z) = z$  and thus  $f(z) = 1$ , as expected. We get even  $y(z) = z - z^3/3$  and  $f(z) = 1 - (10/9)z^2$ , as long as  $z \ll 1$ . When  $z \gg 1$ , it follows from (4) and  $y(z) = 1$  that the asymptotic variation of  $f(z) = 1/3z^2$ . This can also be deduced from (2).

The associated functions  $y(z)$  and  $f(z)$  are represented in **Figure 3**. In the following section, we will compare this empirical mass density distribution for DM in galactic halos to theoretical predictions (**Figure 4**). It would have been useful to compare the function  $\rho(r)$ , which can be directly derived from observations, to results of  $N$ -body computer simulations. When  $x = r/R$ , where  $R$  is a natural unit of length, they can be expressed in the following way

$$\rho_N(x) = \frac{\rho_1}{x(1+x)^2} \quad \rho_B(x) = \frac{\rho_o}{(1+x)(1+x^2)} \quad \text{and} \quad \rho_E(x) = \rho_o \exp(-Ax^\alpha)$$

The first expression was obtained by Navarro, Frenk and White [12] in 1996 and the second one in 1999 by Burkert and Silk [13]. These functions decrease, but the asymptotic variation is  $1/x^3$  instead of  $1/x^2$ . The more general expression  $\rho_E(x)$  was already proposed in 1993 by Einasto [14]. An evaluation by Merritt *et al.* concluded in 2006 that the Einasto profile is the best [15], but for this parametrization,  $A$  and  $\alpha$  depend on the total mass of DM halos [16].

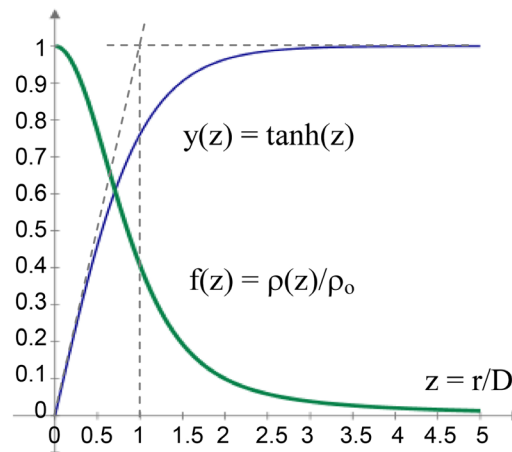


Figure 3. The empirical functions  $y(z)$  and  $f(z)$ .

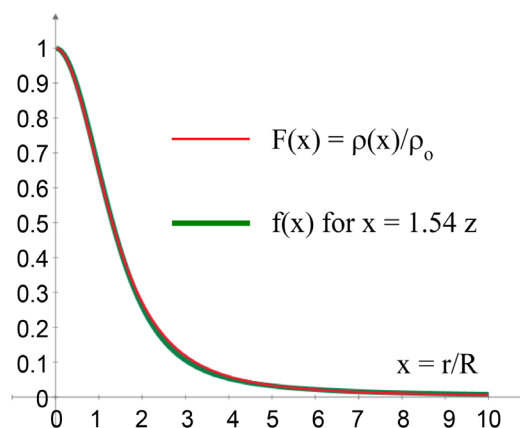


Figure 4. Theoretical and empirical density profiles.

## 2.2. Theoretical Mass Density Profile in DM Atmospheres

We will now compare the empirical profile  $f(z)$ , determined by (4), with a theoretical one. It is deduced from the definition of DM pressure by  $p = nkT$ , where  $n$  is the local density of DM particles and  $3kT/2$  their average kinetic energy. Since DM particles cannot interact with photons and with particles of ordinary matter, local heating is excluded. The cosmic DM gas is *isothermal* in the whole universe and tends to be distributed as evenly as possible. However, it is also gravitationally attracted by the masses  $M$  and  $Mr$ . The relevant force depends on the local mass-density  $\rho = nm$  of the DM gas. It is proportional to the average mass  $m$  of DM particles, but also to their density  $n$ . We get thus  $p = \tau\rho$ , where  $\tau = kT/m$  refers to thermal agitation.

Since gravitational attraction towards the center of the galaxy increases the particle density  $n$ , this increases also the local pressure  $p$ . The cosmic DM gas will thus behave like the air atmosphere of the Earth. Greater pressure at lower altitude, allows for hydrostatic equilibrium. To express this condition for galactic DM atmospheres, we consider again the model of Figure 1. The mass  $\Delta m$  of DM contained in a portion of a very thin spherical layer of radius  $r$  will be attracted

towards the center of the galaxy. For a layer of thickness  $dr$  and a portion that is delimited by a central solid angle  $d\Omega$  this mass is  $\Delta m = \rho(r)r^2 dr d\Omega$ . The radial gravitational force is  $g(r)\Delta m$ , when  $g(r)$  is the local gravitational acceleration, but this force is equilibrated by the difference of pressure forces  $\Omega r^2 p(r)$  exerted on the lower and upper surfaces. Since the pressure decreases when  $r$  increases,

$$g(r)\rho(r)dr = [p(r) - p(r+dr)] = -\frac{dp}{dr}dr$$

Because of  $p(r) = \tau\rho(r)$ , we get a differential equation for  $\rho(r)$ :

$$g(r)\rho(r) = -\tau\frac{d\rho}{dr} \quad \text{or} \quad \rho(r) = \rho_o \exp[u(r)] \tag{5}$$

Galactic DM mass density profiles are always of the Einasto type, but

$$\frac{du}{dr} = -\frac{g(r)}{\tau} \quad \text{or} \quad x^2 \frac{du}{dx} = -3 \int_0^x e^u x^2 dx \tag{6}$$

This follows from (2), where the mass  $M$  is negligible when

$$r = xR \quad \text{where} \quad R^2 = \frac{3\tau}{4\pi G\rho_o} \tag{7}$$

Derivation of the integral Equation (6) yields

$$u'' + \frac{2u'}{x} + 3e^{u(x)} = 0 \quad \text{when} \quad \frac{\rho(x)}{\rho_o} = F(x) = \exp[u(r)] \tag{8}$$

The differential equation for  $u(r)$  can be solved by numerical integration, with the boundary conditions  $u(0) = 0$  and  $u'(0) = 0$ , since  $\rho(r) = \rho_o$  when  $r \rightarrow 0$ . The resulting function  $F(x)$  is represented by the red curve of **Figure 4**. It is practically identical to the green curve for  $f(z)$  when  $z$  is replaced by  $x = \beta z$ , where  $\beta = 1.54$ . The agreement between theoretical and empirical curves validates the concept of DM pressure and STQ. We can even see why  $D$  and  $V$  depend on specific properties of DM particles in different galaxies. Since  $x = \beta z$  implies that  $r/R = r/D$ , it follows from (3) and (7) that  $(D/R)^2 = V^2/\tau = \beta^2 = 2.37$ . The flat rotation curves imply that the value of  $V$  determines the value of  $w = kT/mc^2$ . Because of (3),  $D$  is greater and  $w$  is smaller for low values of  $\rho_o$ .

Actually,  $V^2/3\tau = (V/c)^2/3w \approx 1$ . According to **Figure 2**,  $V \approx 150$  km/s or  $V/c = 0.5 \times 10^{-3}$ . This means that  $w \approx 10^{-7}$ . The cosmic DM gas is cold. If we did know  $kT$ , we could determine the average mass  $m$  of DM particles. Since DM particles cannot interact with photons, they are not in thermal equilibrium with the cosmic microwave background. However, color neutral  $n_e$  marks could be converted into  $\nu_e$  neutrinos [10]. If the cosmic DM gas were in thermal equilibrium with the cosmic neutrino background ( $T = 1.95$  K), the average mass of galactic DM particles would be such that  $mc^2 \approx 3.2$  keV. This figure could be helpful for detecting DM particles.

The results of numerical simulations led to different density profiles  $\rho(x)$ , since they did *not* account for DM pressure. They were based on the Standard

model of cosmology, where it is assumed that DM particles do not interact with one another. The concept of self-interacting DM has been proposed to improve the agreement with observed galactic density profiles [17]. Bullock and his team confirmed this by simulations [18]. STQ explains why DM particles interact with one another and why elastic collisions are predominant in DM atmospheres.

### 2.3. Luminous Matter and Dark Matter

Initially, we thought that the very great mass  $M$  of the central black hole of galaxies is responsible for the attraction of huge amounts of DM and the spherical symmetry of halos for spiral galaxies. Because of (2), it appeared that the actual value of  $M$  is irrelevant. This suggests that a spherically symmetric DM halo could even be *autonomous*. It is sufficient that the central mass density  $\rho_0$  is very great and that the DM atmosphere is not rotating. Actually, there are so-called “voids”, where the density of luminous matter is quite low, but there is DM that could be attracted towards a small local concentration of baryonic matter. Since cosmic DM gas tends to be distributed as evenly as possible, there is no DM void. More and more DM could thus be accumulated, even when there is only a small amount of baryonic matter (BM).

This explains some recent observations. It is now possible, indeed, to localize massive DM halos by gravitational lensing. This led already in 1999 to the discovery of a “truly massive dark clump” in the cluster Abell 1942 [19]. It was said to represent a new class of objects with unusual properties, since the baryon density is there very low [20]. Even a so-called “ghost galaxy” has been detected in 2016 [21]. This Dragonfly 44 galaxy belongs to the Coma cluster and contains nearly no stars. It is “relatively round” and “nearly dark”, although the mass of DM is similar to that of the Milky Way. It seems to be a “failed galaxy”, prevented from building a normal stellar population. Its low luminosity and lack of a classical disk and bulge were said to be “anomalous”, but there are also other faint galaxies in the Coma galaxy cluster.

Dragonfly 44 was said to be “representative of an entirely new class of objects”, indicating that our understanding of the formation of galaxies is not yet sufficiently complete [22]. However, the constitution of spiral galaxies and DM halos will usually result from a synergy, leading to a statistical correlation between the amount of baryonic matter and DM in spiral galaxies. The Tully Fischer relation [23] expresses it in terms of the luminosity  $L$  and the orbital velocity  $V$ .

We mentioned in the introduction the puzzling claim [8] that rotation curves of galaxies seem to be due to baryonic matter alone. Actually, the gravitational acceleration  $g_{\text{obs}}$  was determined by means of rotation curves and compared to an acceleration  $g_{\text{bar}}$  that was calculated by means of the radial variation of the surface brightness of baryonic matter. It appeared that  $g_{\text{obs}}$  and  $g_{\text{bar}}$  were strongly correlated. For large values, they were even equal to one another. This may suggest that the orbital velocity  $V$  does not depend on DM, but  $g_{\text{bar}}$  was calculated by considering a spherically symmetric gravitational potential. Its radial gradient would then determine the centripetal acceleration. However, lu-

minous matter is essentially distributed in the galactic disk and we will show in section 4.1 that gravitational effects are then very different from those of spherically symmetric mass distributions. The existence of DM does not have to be questioned.

### 2.4. The Small Solar DM Atmosphere

The motions of planets in our Solar system were correctly described without considering any DM. The mass  $M_o$  of the Sun is so modest, indeed, that it cannot attract much DM from outer space. Its density  $\rho_s$  is there very low. Nevertheless, the Sun attracted some DM and constituted its own spherically symmetric DM atmosphere. Since it has to be in hydrostatic equilibrium, the mass density  $\rho(r)$  varies according to (5), where  $g(r)$  is defined by (2). However,  $Mr$  is negligible with respect to the mass  $M_o$  of the Sun. Thus,

$$\frac{d\rho}{dr} = -\frac{L}{r^2}\rho(r) \quad \text{and} \quad \rho(r) = \rho_s e^{L/r} \quad \text{where} \quad L = \frac{G}{\tau} M_o \quad (9)$$

The boundary condition is satisfied, since  $\rho(r) \rightarrow \rho_s$  when  $r \rightarrow \infty$ , but this solution is only valid outside the Sun ( $r \geq r_1$ ). Contrary to the air atmosphere of the Earth, the Solar DM atmosphere penetrates into this star. At a distance  $r$  from the center of the Sun, DM is attracted by the mass

$M(r) = (r/r_1)^3 M_o$ , when we consider only the average mass density of baryonic matter inside the Sun. The reduced attraction yields the equation

$$\frac{d\rho}{dr} = -br\rho(r) \quad \text{and} \quad \rho(r) = \rho_{so} e^{-br^2/2} \quad \text{where} \quad b = L/(r_1^3)$$

$\rho_{so}$  is the DM mass-density at the center of the Sun and  $\rho(r)$  decreases like a Gaussian curve inside the Sun. At its surface,

$\rho(r_1) = \rho_{so} \exp(-L/2r_1) = \rho_s \exp(L/r_1)$ . Thus,  $\rho_{so} = \rho_s \exp(3L/2r_1)$ . For the Sun,  $GM_o/c^2 = 1.47$  km. When  $mc^2/kT \approx 10^7$  as for galaxies, the length  $L \approx 1.5 \times 10^7$  km = 0.1 AU. Since  $r_1 = 4.65 \times 10^{-3}$  AU,  $\rho_{so} \approx \rho_s \exp(32)$ . Evaluations of  $\rho_s$  display wide variations [24], but  $\rho_s \approx 10^{-24}$  g/cm<sup>3</sup>. This would yield  $\rho_{so} \approx 8 \times 10^{-11}$  g/cm<sup>3</sup>, while the Sun's average mass density is 1.4 g/cm<sup>3</sup>. The contribution of the solar DM atmosphere to its mass  $M_o$  is negligible.

Pitjec and Pitjeva [25] evaluated the *upper limit* for the DM density  $\rho(r)$ , allowed by present-day measurements when  $r$  is the average orbital radius for Mercury, Venus, Earth, Mars, Jupiter or Saturn. For Mercury ( $r_2 = 0.387$  AU), they found that  $\rho(r_2) < 9.3 \times 10^{-20}$  g/cm<sup>3</sup>. We get  $\rho(r_2) \approx 1.3 \times 10^{-24}$  g/cm<sup>3</sup>. Planetary motions are thus not affected by the mall Solar DM atmosphere.

### 2.5. The Stability of the Oort Cloud

The *Kuiper belt* is composed of small icy objects, orbiting around the Sun in its ecliptic plane between about 30 and 55 AU. It constitutes a reservoir for *short-period comets*, formed about 4.5 billion years ago. They are “fossils” of the origin of the Solar system and some of them can be ejected from the Kuiper belt, because of gravitational interactions with outer planets or mutual scattering.

There are also *long-period comets*, moving around the Sun on very elongated elliptical orbits with an isotropic distribution. They were assumed to come from a spherically symmetric layer, surrounding the Sun between 50 and 100 thousand AU. The average radius of this “Oort cloud” is immense, since the closest star (Proxima Centauri) is situated at 265 thousand AU. How is it possible that the Sun attracted ordinary matter from far away and stored it in a spherical shell?

A constant mass-density  $\rho_s$  of DM would even imply that the total mass  $Mr$  of DM inside a sphere of radius  $r$  increases like  $\rho_s r^3$ . Beyond a certain distance,  $Mr$  would become greater than the mass  $M_o$  of the Sun. More and more DM and BM would be attracted towards the Sun. Actually, the value of  $\rho_s$  that we considered in the previously section, would imply that  $Mr \approx M_o$  when  $r \approx 500$  thousand AU. Inside the Oort cloud, the mass-density of the DM gas remains equal to  $\rho_s$ , but why can baryonic matter be stored in the Oort cloud and remain there in equilibrium?

The spherical Oort cloud protects the Solar system from undesirable intrusions, like the membrane of biological cells. However, the Oort cloud is attracted by the Sun and should collapse. This reminds us of soap bubbles. They should collapse because of surface tension, but this is opposed by a somewhat higher air pressure inside these bubbles than outside. The Oort cloud can be stabilized by DM pressure, since that requires only that the mass density  $\rho_s$  of the DM gas is somewhat higher inside than outside the Oort cloud.

Actually, the DM mass-density decreases progressively from  $\rho_s$  inside the Oort cloud to  $\rho_{is}$  in the surrounding interstellar space, while the mass-density of baryonic matter (BM) increases and decreases there like a Gaussian curve. The associated variations can be determined by considering that BM is embedded in the DM gas, but for our present purpose, it is sufficient to treat the Oort cloud like the liquid membrane of a soap bubble. When the Oort is mentally reduced to a spherical membrane of radius  $r = X$  and small thickness  $\delta$ , every part of it is attracted towards the Sun, but this force is equilibrated by the difference of pressure forces. Equation (5) is then reduced to

$$\frac{GM_o}{X^2} \rho_s \approx \frac{kT}{m\delta} (\rho_s - \rho_{is})$$

### 3. Embedding Dark Matter Atmospheres

#### 3.1. Globular Star Clusters and Elliptical Galaxies

Globular star clusters are spherically symmetric groups of  $10^4$  to  $10^7$  *very old* stars. It is thus astonishing that these stars could remain separated from one another. The astronomer Jeans assumed that these stars are moving around as if they were subjected to thermal agitation. He recognized, indeed, that gravitational interactions between stars should lead to mutual scattering and that their motions will be randomized [26]. He thought that globular star clusters are in hydrostatic equilibrium because of the resulting pressure. This contributes to its stability, but is not sufficient. Since BM can lead to irreversible aggregation, the equilibrium would be unstable.

Globular star clusters are actually situated in galactic DM halos, outside the visible disk. They did thus attract DM and constituted their own DM atmosphere. Although stars and DM are then subjected to common gravitational attractions towards the center of the globular cluster, they would resist collapse by means of *two* different pressure effects. Indeed, Jean's thermal agitation of stars can be combined with DM pressure. The mass density  $\rho(r)$  of the DM gas and the average mass density  $\hat{\rho}(r)$  of ordinary matter vary like  $\rho(r) = \rho_o \exp[u(r)]$  and  $\hat{\rho}(r) = \hat{\rho}_o \exp[u(r)]$ . The central values are different, but the radial distributions are identical. Because of (5),

$$\frac{du}{dr} = \frac{-4\pi G}{r^2} \int_0^r (C + \hat{C}) e^{u(r)} r^2 dr \quad (10)$$

The constant  $C = \rho_o m/kT$  and  $\hat{C} = \hat{\rho}_o \hat{m}/k\hat{T}$ . Setting  $r = x\lambda$  and  $\lambda^2 = 3/4\pi G(C + \hat{C})$ , we get the differential Equation (6). This yields the function  $F(x) = \exp[u(r)]$  of **Figure 4**. The average distribution of visible matter in globular star clusters provides thus an adequate image of the DM profile, but there can be much more DM than BM. Recent observations confirmed that DM is an important component of globular star clusters. ESO's Very Large Telescope in Chile made it possible to analyze 125 compact stellar systems near a giant elliptical galaxy. They suggested also that globular star clusters should have a "significant dark gravitating component" [27].

*Elliptic galaxies* are similar to globular star clusters, but they contain much more DM and stars. Many stars were so strongly attracted towards the *global* center of gravity, that they constituted there a supermassive black hole. Other stars remained in orbit, but not like they do in spiral galaxies. Their motions were constantly perturbed by gravitational interaction. Collapse of this swarm was not only prevented by quasi-thermal agitation. It resulted also from the fact that moving stars were embedded in a DM atmosphere. By participating in the global rotation, it justifies also the spheroidal shape of elliptical galaxies. Recent astrophysical observations confirmed that they are rotating [28] and that there is some kind of "conspiracy" between DM and stars [29].

### 3.2. Cosmic Filaments and Collisions of Galactic Clusters

*Cosmic filaments* are the greatest structures in our Universe. They are composed of galaxies that contain stars and planetary systems, dust and hot gas. These entangled filaments constitute a cosmic web, since they are "knotted" together at places where there are superclusters of galaxies. These filaments are gigantic, but they are also associated with DM. It facilitated their formation and insures their stability. For any rectilinear portion of cosmic filaments and cylindrical coordinates, Equation (10) is replaced by

$$\frac{du}{dr} = -\frac{2\pi G}{r} \int_0^r (C + \hat{C}) e^{u(r)} r dr \quad \text{where } r = x\Lambda$$

Setting  $\Lambda^2 = 3/2\pi G(C + \hat{C})$ , this yields the integral Equation (6). The density distributions of DM and ordinary matter are thus also universal function for cosmic filaments. *Galactic clusters* can contain up to several thousand galaxies.

They are associated with DM, but we recall that the mass  $Mr$  of DM atmospheres can be much greater than the mass  $M$  of BM. Galaxies and galactic clusters are moving. They can even pass through one another or be affected by tidal interactions. These are slow processes on terrestrial timescales, since huge masses imply not only enormous gravitational forces, but also great inertia. It is possible, today, to localize galaxies by means of the emitted electromagnetic radiation and big clumps of DM by means of gravitational lensing, but we get only “snapshots”. It can thus be difficult to distinguish between configurations before or after close encounter. Anyway, DM atmospheres can become autonomous entities. Galactic collisions seem to provide evidence for self-interacting DM [30], but they should be described by pressure effects.

## 4. Rotating DM Rings in the Solar System

### 4.1. Formation of Planetary Systems

The Sun is at least a second generation star. When the initial stars exploded, they dispersed DM as well as BM. Both types of matter were gravitationally attracted towards the center of a new stellar system, but angular momentum had to be separately conserved. Indeed, DM particles do not collide with particles of BM and they tend to be distributed as evenly as possible. This led to the formation of a *protoplanetary disk*, where DM could remain in dynamical equilibrium by means of adequate orbital velocities. We have thus to expect that there is not only a small Solar DM atmosphere, but also a rather great amount of DM that is still orbiting in the ecliptic plane.

A very instructive picture of a *protoplanetary disk* was obtained in 2014 for the HL Tau star by means of ESOs ALMA Telescope [31]. This star is only about 1 million years old and visible matter is still distributed in large circular rings. The formation of planets resulted from gravitational accretion of baryonic matter, with a tendency to be radially distributed according to the Titius-Bode law. It is due to resonance effects for orbital motions at different frequencies [32]. However, DM particles will remain dispersed, because of elastic scattering. This means that DM rings are rotating around the Sun like planets, but they constitute a quasi-continuous radial distribution of the *surface mass-density*  $\sigma(r)$ . Since this function was determined by the conditions that prevailed during the formation of the Solar system, it may reach its maximum value in the region of the big planets, but DM pressure implies that  $\sigma(r)$  becomes only negligible far beyond the Kuiper belt.

Are there signs of the presence of rotating DM rings in our Solar system? They are not obvious, but we know that *asteroids* are relatively small rocky objects, orbiting around the Sun between Mars and Jupiter. They constitute a flat circular belt, extending from about 2.2 to 3.3 AU. To assume that they result from the explosion of a planet is not plausible, since the debris would have been attracted toward a local center of gravity. It is also unbelievable that they were initially distributed in a homogenous way in vacuum, but failed to merge.

Actually, we know that the inner zone of the Solar system allowed for the

formation of compact solid planets, while big gaseous planets were created in the outer zone. The intermediate zone allowed only for the formation of smaller solid objects. Their mutual gravitational interactions were quite modest compared to the stabilizing effect of surrounding DM. Asteroids could thus remain separated from one another, by being embedded in rotating DM rings. They were not only limited to this region, but present everywhere in the ecliptic plane. They stabilized also the *Kuiper belt*, composed of small icy objects.

### 4.2. Gravitational Effects of a DM Disk

The existence of rotating DM rings in the ecliptic plane of the Solar system escaped attention, since their gravitational effects are small and differ from those of customary spherical matter distributions. Any material object that is situated at a distance  $D$  from the center of the Sun would be subjected to the centripetal acceleration  $g(D) = GM_o/D^2$ , where  $M_o$  is the mass of the Sun. It accounts for dynamic stability of planetary motions, but there is also an *additional* radial acceleration  $a(D)$ . It results from all DM rings and its value is

$$a(D) = G \int_0^\infty \sigma(r) f(r, D) dr \quad \text{where} \quad f(r, D) = \int_0^{2\pi} \frac{rd\varphi}{\delta^2} \cos\theta \quad (11)$$

The radial distribution of the surface mass density  $\sigma(r)$  in the ecliptic plane is assumed to be a widely smeared out continuous function. However, every DM ring of radius  $r$  produced a gravitational acceleration at a distance  $D$  from the Sun. The function  $f(r, D)$  specifies its value for one DM ring of radius  $r$ , carrying a constant and unitary mass density when  $G = 1$ . The resulting acceleration is positive like  $g(r)$ , when the probe is attracted towards the center of a smaller circle. It is negative for attraction towards the closest part of any greater circle. Since these effects tend to compensate one another, they are easily overlooked. To calculate  $a(D)$  for a given distribution function  $\sigma(r)$ , we have to know the function  $f(r, D)$ . The angles  $\varphi$  and  $\theta$ , as well as the distance  $\delta$  are defined in **Figure 5**. The triangle yields  $r^2 = \delta^2 + D^2 - 2\delta D \cos\theta$ , where  $\delta^2 = r^2 + D^2 - 2rD \cos\varphi$ . Eliminating  $\cos\theta$ , we get

$$f(r, D) = 2r \int_0^\pi \frac{(D - r \cos\varphi) d\varphi}{(r^2 + D^2 - 2rD \cos\varphi)^{3/2}}$$

The function  $f(r, D)$  can be calculated for any value of  $r$  and  $D$  by means of elliptic functions [33], but numerical integration is sufficient. A typical curve  $f(r, D)$  is represented in **Figure 6**. The values of  $r$  and  $D$  are expressed in arbitrary units, which could thus be AU. The singularity for  $D \approx r$  is obvious, since the test object would then be strongly attracted by the nearest parts of the ring, as if it were a straight line. Since  $1/(D - r)$ , DM rings have thus long-range effects, although the surface mass density  $\sigma(r)$  may be quite small and can lead to compensation of attractions towards the Sun and away from it. At the center of any DM rings,  $f(r, 0) = 0$ , while far away, it acts as if its total mass were concentrated at its center. Thus,  $f(r, D) \rightarrow 2\pi/D^2$  when  $D \gg r$ .

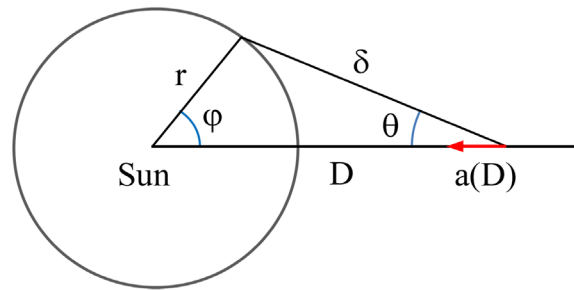


**Figure 5.** Gravitational attraction by a single ring of DM.

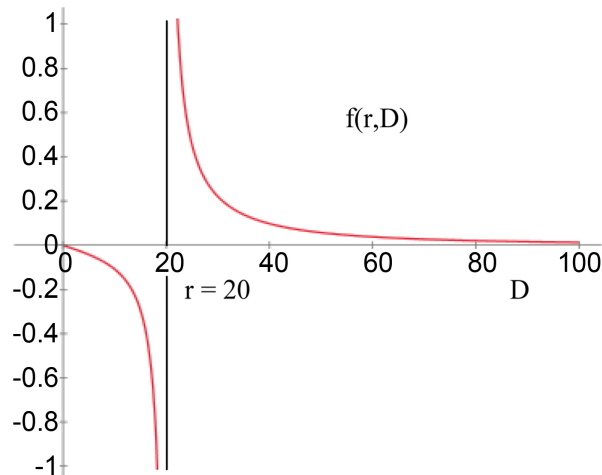


**Figure 6.**  $f(r, D)$  for a DM circle of radius  $r = 20$ .

### 4.3. The Perplexing Pioneer Anomaly

Telemetric measurements of the velocity of the Pioneer 10 and Pioneer 11 spacecraft revealed a small deceleration when they were moving away from the Sun [34]. This is equivalent to an additional positive acceleration, oriented towards the Sun. It was unexpected and thus said to be “anomalous” with respect to Newton’s law of gravity. When this result was published in 1998, simple causes and conceivable errors were discarded. Similar effects were even reported for other spacecraft. **Figure 7** shows that the anomaly was detected for Pioneer 11, after its flyby of Jupiter ( $D = 5.2$  AU) and Saturn ( $D = 9.6$  AU). It increased up to the orbit of Uranus ( $D = 19.2$  AU) and remained then nearly constant. The same value was also found when measurements were started and pursued for Pioneer 10, but there was then a slight decrease.

Unfortunately, the so-called “onset” of the Pioneer anomaly was only observed for Pioneer 11. Since Pioneer 10 had been launched *one year earlier*, its anomalous acceleration had not been noticed and was only measured for this spacecraft when  $D > 25$  AU. Although the onset is a prominent feature of **Figure 7**, attention was only focused on the plateau. It was stated in 1998 that the “canonical” value of the anomalous acceleration is  $8.74 (\pm 1.33) \times 10^{-10} \text{ m/s}^2$  [35]. This value applies to both spacecraft and the essential problem was to decide between two possibilities.

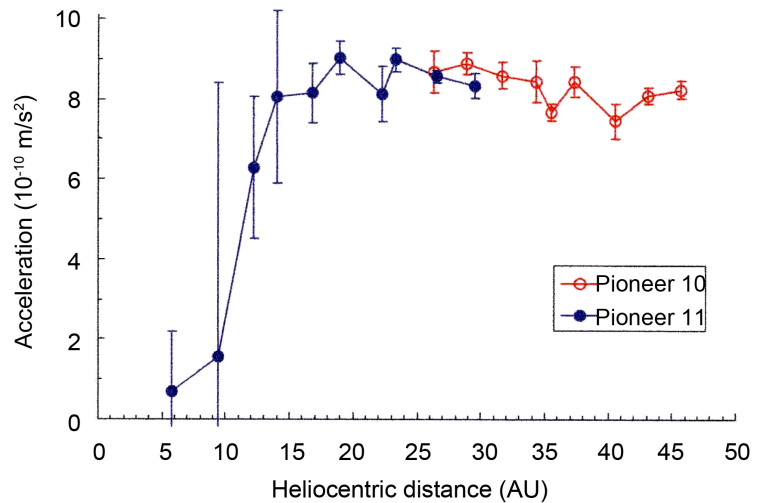


**Figure 7.** The “onset” of the Pioneer anomaly. The anomaly was not immediately noticed for Pioneer 10.

Does the anomaly result from a force of external origin that is directed towards the Sun, or should it be attributed to a small braking force, produced by the spacecraft themselves. Being aware of the possible existence of rotating DM rings in the ecliptic plane, we wanted to see if this hypothesis could explain the Pioneer anomaly. We developed thus the theory of the preceding section and calculated  $a(D)$  by means of (11) for various distributions  $\sigma(r)$ . It appeared that the “onset” could easily be explained by nearly equal gravitational attractions towards smaller and greater DM rings. They tend to compensate one another until the inner DM rings attract more than the remaining outer rings. **Figure 8** shows the result for the indicated distribution  $\sigma(r)$  when  $G = 1$ . To perform the numerical integration in a simple way, we superposed here only two Gaussian curves, respectively centered at  $r = 5$  and  $r = 15$ , with a width of 200 and 2000 and a central magnitude of 1.7 and 2.3. Since these distances could be expressed in AU,  $\sigma(r)$  displays a broad maximum near the orbits of the great planets and vanishes only far beyond the Kuiper belt.

The Pioneer 10 and 11 spacecraft had been constructed in exactly the same way and they carried two external  $\text{Pu}^{238}$  radioisotope power sources. The possibility of anisotropic heat radiation had been examined and rejected [34], but a short comment of Katz [36] stated that this effect might have been “underestimated”. The NASA specialists answered [37] that enough power was available, but that the design and position of the power sources would not allow for sufficiently strong heating and anisotropic radiation of the large antenna. These sources “see” it edge on. Nevertheless, the hypothesis of a *purely thermal effect* came more and more in vogue.

An estimation of thermal effects by means of model calculations was published in 2008. It was asserted that recoil of IR photons could account for 35% to 57% of the canonical value [38]. This result was considered as providing “a clear indication of the *possible* thermal origin of the so-called Pioneer anomaly”. In

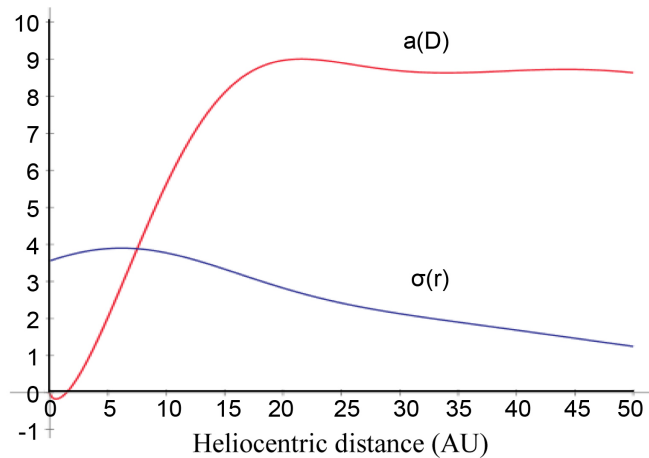


**Figure 8.** Calculated acceleration  $a(D)$  and mass density  $\sigma(r)$ .

April 2012, the same authors included also diffuse reflection. This accounted for 26% - 66% of the plateau [39]. The “onset” was disregarded and the slow decrease of the anomaly was attributed to the radioactive decay of the  $\text{Pu}^{238}$  power sources. Rievers presented in January 2012 his doctoral thesis [40], where he claimed that thermal effects “can explain the so-called Pioneer anomaly within a modeling accuracy of 11.5%”.

In April 2012, Turyshev *et al.* published the result of their own computations, based on a comprehensive model of Pioneer 10 and 11 and data available at the JPL. Evaluating thermal effects at various heliocentric distances, they found that the numerical estimate of the recoil force amounts to about 80% of the measured values [41]. However, they stated that “once the thermal recoil force is properly accounted for, no anomalous acceleration remains” and concluded even that the Pioneer anomaly “is consistent with *known physics*.” Another computation [42], published in July 2013, strengthened the conviction that “solutions may be achieved that do not require the addition of any ‘unknown’ acceleration other than the one of thermal origin.”

The desire to stick to a conventional explanation was noticeable, but it could be misleading, since thermal modeling depends on many factors and no calculation did account at least for 100% of the canonical value. Moreover, the back-scattering of thermal radiation could not suddenly start and increase for Pioneer 11 between 5 and 20 AU. Solar radiation pressure varies also in a smooth and predictable way. To prove or disprove the reality of the “onset” of the anomalous acceleration could have been decisive. Turyshev and his colleagues had recuperated initial data in 2005, but did not report that this input eliminated the threshold [43]. There remained uncertainties.

Since the author of this article had developed the theory of DM rings in 2012, he asked (by email on Dec. 3, 2012) if the onset was still there. Having calculated the acceleration  $a(D)$  and found results like that of **Figure 8**, Meessen mentioned that rings of DM particles, rotating around the Sun in its ecliptic plane can explain the onset of the Pioneer anomaly and also the decrease of  $a(D)$

between 20 and 45 AU. Slava Turyshev kindly answered that the onset subsists and confirmed that the decrease of the anomaly does not agree with the radioactive lifetime of the  $\text{Pu}^{238}$  energy source. He attributed this discrepancy to electronic parts of the energy conversion system. The author waited for proofs of a purely thermal effect by means of laboratory experiments, but the problem seemed to be settled, at least for public opinion.

#### 4.4. Why Are Planets Not Affected?

Checking then the literature in regard to DM rings, we found that Moore and Moore [44] had also considered the gravitational effect of a DM distribution  $\sigma(r)$  in the ecliptic plane of the Solar system. They had even determined the function  $\sigma(r)$ , which yields the *closest match* with Figure 7. It is very similar to  $\sigma(r)$  in Figure 8. These authors solved also another problem, at least partially. The motion of planets has been correctly described without considering any DM. We have shown in section 2.4 that the spherically symmetric Solar DM atmosphere is too small to influence the motion of planets, but why are they not perturbed by rotating DM rings? If the acceleration  $a(D)$  reported in Figure 7 were due to some additional gravitational force, oriented towards the Sun, it should have been noticed. This was proven in 2006 by Iorio and Guidice [45]. They found that the orbital motions of Uranus, Neptune and Pluto would have been perturbed, but this has not observed. Tangen [46] confirmed.

Moore and Moore showed that these planets are protected when they create *deep trenches with steep walls* in the DM distribution  $\sigma(r)$ . Because of the singularity of the function  $f(r, D)$ , represented in Figure 6, the acceleration  $a(D)$  would then display two sharp peaks of opposite sign at the inner and outer walls of such a trench. In the middle, the dominant attraction towards the closest inner and outer DM rings would compensate one another. This was said to yield “gravitational nulls”. It is thus possible to justify that  $a(D) \approx 0$  for these planets, but why should there exist a gap in the distribution of rotating DM rings, precisely where the planets are?

We propose a mechanism that explains this apparently exotic assumption. Any planet attracts DM particles in its immediate vicinity. It creates thus a local void, but DM particles tend to be distributed as evenly as possible, because of mutual scattering. However, they have also to remain on the same orbit to insure dynamic equilibrium. They will thus move towards the planet along their normal orbit. Eventually, there remains a gap in the radial distribution of the DM mass-density distribution  $\sigma(r)$  exactly on the orbit of the planet and close to it. Is this true? A visual proof is provided by a picture of Saturn’s small moon Daphnis [47]. It is orbiting inside a circular gap of the visible rings. This confirms our proposition that asteroids and objects of the Kuiper belt are embedded in DM rings, rotating around the Sun. Saturn’s famous rings confirm also that small objects remained distributed in rotating DM rings.

We can now use Figure 8 to estimate the surface mass-density  $\sigma(r)$  of DM in the ecliptic plane. Since we get about the same value for  $a(D)$  as the ob-

served one when  $\sigma(r) \approx 3$  for  $r \approx 20$  AU and  $G = 1$ ,  $\sigma \approx (3/G)10^{-10}$  m/s<sup>2</sup>. Since  $G = 6.8 \times 10^{-11}$  m<sup>3</sup>/s<sup>2</sup>kg, this yields  $\sigma \approx 5$  kg/m<sup>2</sup>, which is not negligible. It would thus be useful to *launch another spacecraft* to find out if the onset and other features of **Figure 7** are reproduced or not. This could also help to solve other basic problems. The Solar system presents indeed several gravitational anomalies [48] [49] [50]. It is known, for instance, that the distance between the Earth and the Sun is increasing at about 15 m/century [51]. This *secular increase of the astronomical unit* could be due to a small negative value of the acceleration  $a(D)$  when  $D \approx 1$ . This appears in **Figure 8**, but would mean that the Earth is not sufficiently protected, although it creates also a circular gap in the DM density  $\sigma(r)$ . The global effect of all greater DM rings is somewhat stronger than that of smaller ones.

#### 4.5. The Flyby Anomaly

If the Earth did really sweep up all DM that was close to its orbit, its center would be surrounded by rotating DM rings. They are invisible and we ignore their actual distribution. Since the Earth captured DM particles that were moving with respect to the center of the Earth and are not subjected to friction, they constitute a rotating DM disk. It is situated in the equatorial plane, since it is gravitationally coupled to the spheroidal shape of the Earth. DM particles will then be in dynamical equilibrium when they are orbiting at the adequate speed with respect to the center of the Earth. Is there any evidence of such a DM disk?

It does exist, but was too unexpected to be considered at least as a possible cause of a small, but detectable anomaly. According to Newtonian gravity, a spacecraft that is approaching a planet from far away, it will turn around it on a hyperbolic path in the reference frame where the planet is at rest. The speed of the spacecraft has the same value  $V$  when it enters and leaves the sphere of gravitational influence of the planet. This symmetry is broken in the heliocentric frame, since the planet is orbiting around the Sun. The spacecraft can then acquire a higher velocity. This “gravity assist maneuver” is very useful and the result is exactly predictable, but during the Earth flyby of the Galileo spacecraft in December 1990, there appeared an unexpected velocity increase  $\Delta V$ . Other *flyby anomalies* were also detected. The values of  $\Delta V$  could be positive or negative. The greatest one (13.46 mm/s) was observed for NEAR (Near Earth Asteroid Mission). Only 6 Earth flyby anomalies were known in 2009, but Anderson *et al.* [52] recognized a trend:

$$\Delta V = KV\Delta_1 \quad \text{where} \quad \Delta_1 = \cos \delta_1 - \cos \delta_2 \quad (12)$$

$K$  is a constant, when  $\Delta V$  is proportional to  $V$ . The angles  $\delta_1$  and  $\delta_2$  are the declinations of the asymptotes for the arriving and departing spacecraft. They are equivalent to latitudes, but a spacecraft should not be affected by the rotation of the Earth. It follows from (12) that it is irrelevant whether the spacecraft approaches the Earth and leaves it above or below the equatorial plane. However,  $\Delta V$  is positive and greater when the spacecraft is approaching closer to the equatorial plane than when it is leaving. This suggests that there is some-

thing in the equatorial that attracts the spacecraft at grazing incidence. The spheroidal shape of the Earth is not sufficient to explain the anomaly. Could it be due to the equatorial DM disk? **Figure 9** and **Figure 10** provide the answer in terms of a simple model.

**Figure 9** shows the hyperbolic path of a spacecraft in the geocentric system and the angles  $\delta_1$  and  $\delta_2$ . A spacecraft of mass  $m$  is then not only subjected to the gravitational force  $GmM/r^2$  exerted by the mass  $M$  of the Earth, but also to the gravitational attraction of the ensemble of DM rings. For any given declination  $\delta$ , it is equivalent to the additional attraction exerted by two identical masses  $\mu$ . They are situated at a distance  $s$  from the center of the Earth along the azimuth of the spacecraft (insert of **Figure 9**). When the spacecraft is far away, its distance  $r$  to the central mass has to be replaced for the masses  $\mu$  by  $d_{\pm} = r \pm s \cos \delta$ . The gravitational force acting on the spacecraft is thus

$$F(r) = Gm \left( \frac{M}{r^2} + \frac{\mu}{d_+^2} + \frac{\mu}{d_-^2} \right) \text{ where } \frac{1}{d_{\pm}^2} = \frac{1}{r^2} (1 \pm \epsilon \cos \delta)^{-2}$$

For  $\epsilon = s/r \ll 1$  and  $m \ll M$ , we get a second order correction:

$$F(r) = \frac{Gm}{r^2} (M + 3\mu\epsilon^2 \cos^2 \delta) \text{ where } \delta = \delta_1 \text{ or } \delta_2$$

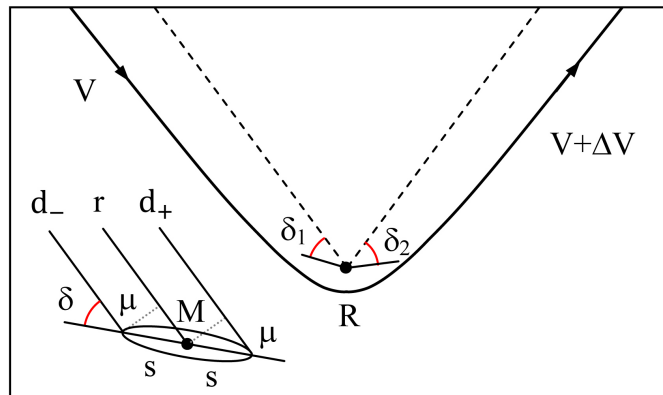


**Figure 9.** Flyby for a planet with a DM ring (see text).

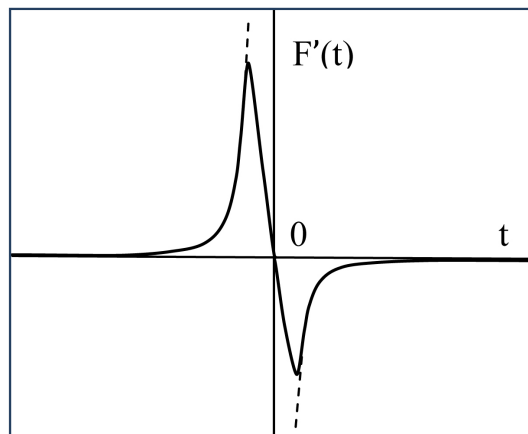


**Figure 10.** Force causing the flyby anomaly.

When the spacecraft is relatively close to the Earth, it is necessary to consider triangles instead of parallel lines and  $d^2 = r^2 + s^2 - 2sr \cos \delta$ . However, the spacecraft would be submitted to the same force  $F(r)$ . It acts like a central force, but the magnitude of the perturbation is

$$F'(t) \approx \frac{Gm}{r^4} 3\mu s^2 \cos^2 \delta \quad \text{so that} \quad m\Delta V(t) \approx \int_{-\infty}^t F'(t) dt \quad (13)$$

The force  $F'(t)$  decreases like  $1/r^4$  instead of  $1/r^2$  and the spacecraft is attracted as long as it is approaching, while it is decelerated when it is leaving. **Figure 10** illustrates the variation of  $F'(t)$ . It is maximal near the point of closest approach, but it changes sign and does not vary in a symmetrical way when  $\delta_1$  and  $\delta_2$  are different. The global result will be accelerating when  $\delta_1 < \delta_2$ . The second relation (13) is based on the simplifying assumption that the perturbing central force is acting along the asymptotes of the hyperbolic path of the spacecraft. This is not true near the turning point, but the perturbation will then usually be negligible. The integral can be evaluated, since  $r = r(t)$  and  $dt \approx dr/V$ . The modification of the orbital velocity  $v(r)$  remains small:

$$\Delta V \approx \frac{3G\mu s^2}{V} \int_R^{\infty} \frac{dr}{r^4} \Delta_2 = \frac{K'}{VR^3} \Delta_2 \quad \text{where} \quad \Delta_2 = \cos^2 \delta_1 - \cos^2 \delta_2 \quad (14)$$

The constant  $K' = G\mu s^2$  depends only on intrinsic properties of the DM rings. It is identical for all Earth flybys. The distance  $R$  of closest approach is an essential parameter, since there will be no flyby anomalies when  $R \gg s$ . This did not appear in (12). The dependence on the velocity  $V$  is also different. Actually, the flyby anomaly has to increase for a slower spacecraft, since it is exposed during a longer time to the accelerating and decelerating forces. The declinations  $\delta_1$  and  $\delta_2$  do also have different effects, but Anderson and Nieto [52] deduced already from a small set of measurements that the velocity increase depends on  $\cos \delta_1$  and  $\cos \delta_2$ . Jouannic *et al.* tried to find “potential causes” of the flyby anomaly by means of a statistical analysis [53]. Their empirical law was identical to (12) when  $K$  is inversely proportional to the mass  $m$  of the spacecraft and to the height  $h$  of the perigee above the surface of the Earth.

**Table 1** is based on data extracted from NASA’s Horizon’s web interface [54]. Only the values  $\Delta V_{\text{obs}}$  for the reported flyby anomaly were taken from the initial report [52] and for Cassini, from the later compilation [53]. It should be noted that correlations do not yield causal relations, but the height  $h$  of the perigee above the surface of the Earth was an essential factor. It accounted at least approximately for the fact that no anomaly was observed for recent Earth flybys, as indicated in the column  $\Delta V_{\text{obs}}$  of **Table 1**. We calculated the values of  $\Delta V$  and  $\underline{\Delta V}$  by means of (12) and (14), where the constants  $K$  and  $K'$  were chosen to get agreement with  $\Delta V_{\text{obs}}$  for NEAR. It was not possible to measure the expected flyby anomaly for Juno, since this craft went itself into “save mode”.

The proposed theoretical law (14) provides better agreement with observed values than (12), especially when the spacecraft passes far away from the Earth.

**Table 1.** Parameters for Earth flybys and the corresponding values of the observed velocity increase, while  $\Delta V$  and  $\underline{\Delta V}$  are calculated ones.

Spacecraft (and pass)	Flyby (y.m.d)	$R$ (km)	$V$ (km/s)	$\delta_1$ (°dec)	$\delta_2$ (°dec)	$\Delta V_{\text{obs}}$ (mm/s)	$\Delta V$ (mm/s)	$\underline{\Delta V}$ (mm/s)
Galileo-1	90.12.08	7340	8.9	12.8	-34.0	3.92	4.08	2.98
Galileo-2	92.12.08	6682	8.9	34.0	-5.0	-4.6	-4.67	-4.55
NEAR	98.01.23	6910	6.9	21.0	-71.8	13.46	13.46	13.46
Cassini	99.08.18	7574	16.0	12.9	-5.0	-0.5	-1.06	-0.24
Rosetta-1	05.03.04	8338	3.9	2.4	-34.4	1.80	2.13	5.54
Messenger	05.08.02	8714	4.1	-31.4	-31.8	0.02	0.05	0.01
Rosetta-2	07.11.13	11,685	9.5	10.5	18.0	0	0.95	0.16
Epoxi-1	07.12.31	21,943	3.6	4.0	15.7	0	0.05	0.07
Epoxi-2	08.12.29	49,828	3.6	-21.0	59.0	0	0.47	0.05
Rosetta-3	09.11.13	8862	9.4	-18.5	+24.4	0	1.12	0.42
Epoxi-3	09.06.29	1,336,675	1.5	+4.0	-49.0	0	1.61	$6 \times 10^{-6}$
Epoxi-4	09.12.28	1,325,441	1.1	-40.0	4.0	0	-0.80	$-6 \times 10^{-6}$
Epoxi-5	10.06.27	36,860	3.5	60.2	-17.0	0	-5.05	-0.15
Juno	13.10.09	6947	10.4	-14.2	39.5	-	6.47	3.90

The main discrepancy is observed for Rosetta-1. It could result from a more dissymmetric transition from positive to negative values in **Figure 10** when  $V$  and  $\delta_1$  are small. Since  $K = G\mu s^2 \approx 3.96 \times 10^{13} \text{ km}^3 (\text{km/s})^2$ , it appears that  $s^2 \mu = 5 \times 10^{23} \text{ m}^2 \cdot \text{kg}$ . We ignore the values of  $s$  and  $\mu$ , but the radius of the Earth is close to 6400 km. For  $s \approx 10,000 \text{ km}$ , we would get  $\mu \approx 5 \times 10^9 \text{ kg}$ , while the mass of the Earth  $M \approx 6 \times 10^{24} \text{ kg}$ . Nevertheless, the presence of DM rings rotating around the center of the Earth is detectable.

We add three remarks. 1) The DM disk of the Earth is probably smaller than the orbit of the Moon ( $r = 385,000 \text{ km}$ ), but the Moon and satellites that are moving on smaller circular orbits in the equatorial plane of the Earth would create a circular groove in the DM disk. 2) The flyby anomaly and the Pioneer anomaly apply to unprotected spacecraft. 3) Adler tried already to explain the flyby anomaly by considering the possible existence of a DM disk in the equatorial plane of the Earth [55]. However, he assumed that DM would interact with nucleons of the spacecraft, which is negligible [10]. Here, we considered only gravitational interactions.

#### 4.6. Global Positioning Satellites

Ben Harris concluded from a high-precision study of the motions of GPS, Galileo and GLONAS satellites that the mass of the Earth is 0.005% to 0.008% greater than the value established by the International Astronomical Union [56]. It has been stated [57] that he attributed this effect to the presence of a “disk of DM

around the equator 191 km thick and 70,000 km across". The relevant observational data and the calculations were not published, but it is not sufficient to object that "thin disks like that are generally the result of rapid rotation, while gravity tends to make things spherical" [58]. DM rings are possible.

Moreover, GPS satellites are orbiting around the Earth on circular orbits of radius  $r$  and specific inclinations (like  $55^\circ$ ) with respect to the equatorial plane of the Earth. The declination  $\delta$  will thus vary and the velocity  $v = v(r, \delta)$ . According to (13), the additional central force would vary like  $\cos^2 \delta$ . Since the average value is positive, it accounts for the apparent increase of the mass  $M$  of the Earth. If these satellites were passing through the equatorial DM disk, they would even be accelerated just before entering it and decelerated just after leaving it. The velocities  $v = v(r, \delta)$  could thus reveal special effects when  $\delta = 0$ . When no singularity is observed near the equatorial plane, when  $r = 26,600$  km for instance, this would mean that the DM disk is smaller. A detailed study of the orbital motions of GPS satellites should thus be encouraged.

## 5. First Direct Detection of DM Particles

### 5.1. The Annual Modulation Signature

In the context of present day uncertainties about the nature and properties of DM particles, any direct detection of DM particles would be very important. Nevertheless, we have to proceed by trial and error. In general, it has been assumed that DM particles can interact with nucleons, but we have shown [10] that this is very rare. Even the most sophisticated system that was based on this assumption did not succeed [59]. Since it was not obvious what method should be used, it was suggested already in 1986 to verify if "detected" signals are genuine or not. They should display an *annual modulation* [60]. Indeed, the Sun is moving at about 230 km/s with respect to the galactic DM atmosphere, while the Earth is orbiting around the Sun at about 30 km/s. The flux of DM particles should thus vary every year in a specific way. This would yield at least a "significant enhancement of signal-to-background ratio".

Fortunately, the orbit of the Earth around the Sun is not perpendicular to the "wind" of DM particles. It is inclined by about  $62^\circ$  with respect to the galactic disk. Moreover, the flux should be maximal on about June 2<sup>nd</sup> and minimal close to December 2<sup>nd</sup>. The detection rate has even to vary according to a perfect cosine function, whatever the nature of DM particles may be. It is required, however, that DM particles can be detected by the chosen method and that other possible causes of annual modulations have been excluded. In terms of these criteria, the DAMA (Dark Matter) experiment, installed in the Gran Sasso Tunnel near Rome, did succeed.

This laboratory is situated at about 1400 m under rocks and NaI(Tl) scintillators were chosen to detect galactic DM particles. First results were published in 2003 and provided already evidence of 7 annual cycles [61]. Using 9 very pure and well-protected crystals, the photomultipliers did yield a modulated counting rate. The ensemble of nearly 100 kg NaI crystals was then replaced by about 250

kg. Every one of the 25 scintillators in a protected  $5 \times 5$  arrangement was coupled to a pair of photomultipliers. They had to respond in coincidence, to insure detection of DM particles by means of the flash of light that they produce when they are passing through a particular crystal. The initial results were confirmed. Annual modulation for 14 cycles led to a  $9.3\sigma$  confidence level [62].

The team leader Rita Bernaby and her collaborators insisted in various publications on the fact that detection occurred in a narrow energy range (2 - 6 keV). At slightly higher energies (6 to 14 keV), the annual modulation did not appear anymore. The energy calibration was regularly controlled by means of  $x$ -rays. No systematic process or other side effect could explain the ensemble of observed facts. The signature of a true detection of galactic DM particles is “stringent and unambiguous”, but why was this method successful?

## 5.2. The DM-Electron Interaction

The DAMA team had chosen NaI(Tl) scintillators. Although the nature of DM particles was unknown, it had thus been assumed that a DM particle that passes through a particular crystal might excite there sufficient electrons to get a detectable light flash. Bernaby and collaborators analyzed this process in 2007. They assumed that electrons might be liberated from atoms, as for ionization processes [63]. It seemed important that electrons are not at rest in their initial state, while DM particles were considered as having some great mass ( $\sim \text{GeV}/c^2$ ). The liberated electrons would then have very low energies, with a threshold effect. Similar and more sophisticated investigations followed in 2014 and afterwards [64]. We want to show here that *DM-electron interactions* are possible because of STQ (Figure 11) and that detection by NaI scintillators involves not only elastic collisions, but also some solid state physics (Figure 12).

Figure 11 indicates that a nark  $n_e$ , which could belong to any DM particle, can for instance be in the  $\bar{R}G$  state. Its  $(u_x, u_y, u_z)$  quantum numbers are then  $(1, -1, 0)$ , while  $u_{ct} = 0$  [10]. This nark can change its color by creating a gluon, which is immediately annihilated, by recreating a nark in the initial color

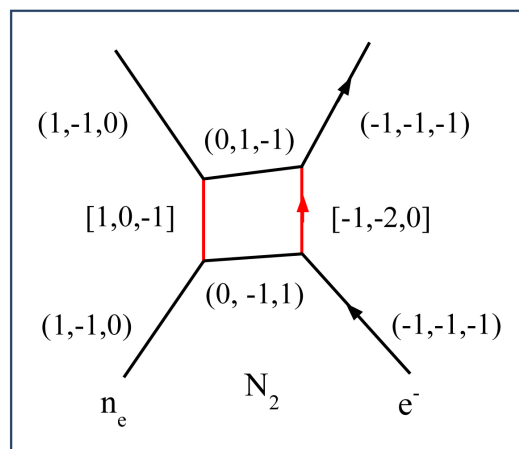
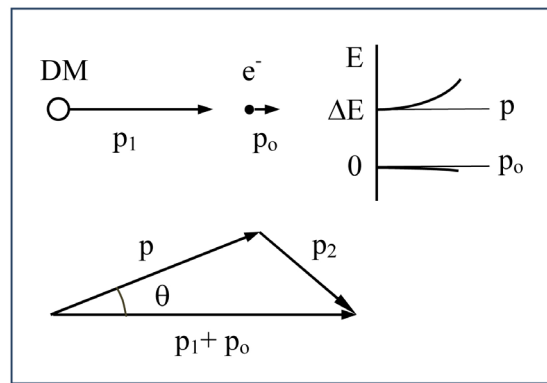


Figure 11. DM-electron interaction is mediated by an  $N_2$  boson.



**Figure 12.** Momenta and possible energies, before and after an elastic DM-electron collision.

state and the antiparticle of the first emitted one. This yields an  $N_2$  boson, which is the mediator for interactions between DM particles, but also between DM particles and electrons. Indeed, an electron can annihilate the emitted particle to create a boson, which is the *supersymmetric partner of an excited electron*. Its charge  $Q = -1$  and its mass could be relatively small, like the mass of an electron. This boson merges with the other member of the  $N_2$  boson, to recreate an electron. STQ accounts thus for elastic scattering of an electron by DM particles.

The upper left part of **Figure 12** represents a DM particle and its initial momentum vector, as well as the initial momentum of one electron. We assume here identical orientations, but it will turn out that this is irrelevant. The mass  $M$  of the galactic DM particle is unknown, but it is moving at least at 200 km/s with respect to the detector. Its initial momentum  $p_1$  should thus be very great with respect to the momentum  $p_0$  of the electron in its initial state. This electron will be scattered by some angle  $\theta$  and acquire a momentum of magnitude  $p$ . The DM particle is also scattered. The lower part of **Figure 12** represents the vectorial momentum conservation law. The momentum of the DM particle changed from  $p_1$  to  $p_2$ , where

$$p_2^2 = p^2 + (p_1 + p_0)^2 - 2p(p_1 + p_0)\cos\theta \quad (15)$$

NaI crystals are insulators. They are excellent detectors for gamma rays, which create or liberate rather energetic electrons. For detection, it is sufficient that they excite electrons from the valence band to the conduction band of the NaI crystals. They will then move as free particles and be rapidly trapped in excited states of dispersed Tl atoms. These centers of luminescence allow for electronic transitions that yield detectable photons. The excitation of electrons and light emission occurs very rapidly and yields discrete scintillations, although many excited electrons were involved. The pulse height is even proportional to the energy of the incident particle.

DM particles can only be detected by this method when they transfer sufficient energy to electrons at the upper boundary of the valence band ( $E = 0$ ) to reach the conduction band. Their energy is then  $E = \Delta E + p^2/2m$ , as indicated

in the upper right part of **Figure 12**. The minimal excitation energy has thus to exceed the band gap  $\Delta E$ . Setting  $\Delta E = P^2/2m$  and  $\mu = m/M$ , energy conservation is expressed by

$$P^2 + p^2 = \mu(p_1^2 - p_2^2) \quad (16)$$

Since  $m \ll 1$  and  $p_1 \gg p_o$ , it follows from (15) and (16) that

$$p^2 - 2\mu pp_1 \cos \theta + P^2 = 0.$$

Solving for  $p$  before considering equally probable angles  $\theta$ , we get

$$p^2 = \frac{\mu^2}{2} p_1^2 - P^2 \quad \text{or} \quad E_e = \frac{m}{2M} E_1 - \Delta E$$

The kinetic energy of the excited electron  $E_e = p^2/2m$  results only from the transfer of a small part of the kinetic energy  $E_1 = p_1^2/2M$  of the DM particle. It can excite many electrons, when the band gap  $\Delta E$  is not too great. This can produce an intense scintillation, comparable to that of  $x$ -rays of relatively low energy (2 - 6 keV). For NaI crystals,  $\Delta E = 5.8$  eV, while  $\Delta E = 6.3$  eV for CsI crystals [65]. The “Korea Invisible Mass Search” (KIMS) tries to detect DM particles by means of CsI(Tl) scintillators. They are less hydroscopic, but seem to be less effective. The flash of light could be weaker for the same type of DM particles or only some of them might be detected. The “Coherent Germanium Neutrino Technology” (CoGeNT) in Minnesota was intended to detect DM particles by means of nuclear recoil, but a modest annular modulation was reported [66]. It can be attributed to DM-electron interactions.

### 5.3. Detection of Galactic DM Signals

We mentioned and discussed the detection 130 GeV gamma-rays by means of NASA’s Fermi telescope and proposed a mechanism for the production of energetic photons according to STQ [10]. However, there is also an  $x$ -ray signal at about 3.5 keV. It was detected by means of the XMM-Newton  $x$ -ray telescope of the European Space Agency and by NASA’s Chandra  $x$ -ray observatory [67]. It is a very weak signal, but it appeared in stacked spectra of 73 galaxy clusters with various redshifts. Dark matter could thus be considered as the possible cause. The XMM-Newton telescope detected these  $x$ -rays for the Andromeda galaxy and the Perseus cluster, with a  $4.3\sigma$  confidence level [68]. The 3.5 keV  $x$ -ray line was also detected for the center of the Milky Way [69], but not for the Virgo cluster. The signal was not “clear” enough.

Moreover,  $x$ -rays can also result from electronic transitions when highly ionized atoms capture electrons from hydrogen atoms. However, the strongest objection resulted from the measurement of the distribution of  $x$ -ray sources at 3.5 keV in the Perseus cluster and near the center of the Milky Way. These sources did not display the radial symmetry, expected for galactic DM density profiles. There were radial and azimuthal irregularities [70]. The spatial distribution of  $x$ -rays sources at neighboring energies (between 2 and 5 keV) displayed also ir-

regularities. Plasma emissions, due to charge transfer for highly ionized atoms, are thus very probable for these sources. Moreover, it has now been experimentally proven that that  $S^{15+}$  and  $S^{16+}$  ions capture electrons and emit  $x$ -rays near 3.4 eV [71]. The proposition that the 3.5 keV signal results from DM is questionable.

Nevertheless, skepticism should be omnidirectional. We mention 4 reasons to be prudent. 1) The detected irregular distribution of  $x$ -ray sources could result from electronic transitions, while DM signals at 3.5 eV were too weak to establish a map. 2) Since they were absent for the Virgo cluster and are always weak, they could be produced only by a particular type of DM particles. 3) The mass-density distribution  $\rho(r)$  is spherically symmetric for DM atmospheres, but it does not distinguish different types of DM particles from one another. 4) We know that they are possible [10] and galactic DM atmospheres could result from gathering clouds of DM particles of different composition. Although mutual scattering of DM particles tends to produce a homogeneous mixture, this takes time and the relevant space is immense.

Could the 3.5 keV  $x$ -ray signal be produced by at least one particular type of DM particles? **Figure 13** shows a process that could be considered for DM particles of type  $N_1$ . They were produced during the Big Bang and should still be present in our universe [10] [11]. They correspond to single marks in the (0,0,0) color-neutral state. Two  $N_1$  particles could thus meet one another and be transformed into a color-neutral gluon. According to the conservation law for  $u$ -quantum numbers, this would allow for  $[0,0,0] \rightarrow (1,1,1) + (-1,-1,-1)$ . The resulting electron-positron pair can yield two photons. We ignore if this process made it possible to detect 3.5 keV photons, but if this were true  $N_1$  DM particles would have this energy. Incidentally, we found the same magnitude for the average mass of galactic DM particles (Section 2.2). It was even suggested by the DAMA team (Section 5.1). Since fusion of DM particles reduces their energy [11], the possible detection of a galactic DM signal at 3.5 keV merits further studies.

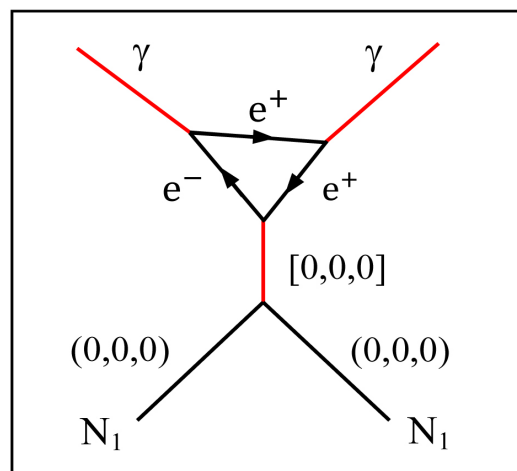


**Figure 13.** STQ could account for transformations of  $N_1$  dark matter particles into a pair of photons.

## 6. Conclusions

The existence of a space-time continuum seemed to be obvious, but this conviction was based on a questionable assumption [10]. We constructed thus a theory of *space-time quantization* (STQ), where the value  $a$  of the ultimate limit for the smallest measurable length was treated as a yet unknown parameter. It appeared that there are no logical inconsistencies when  $a \neq 0$  and that this is sufficient to account for the Standard Model of elementary particle physics. The agreement with numerous and varied observations allows us to conclude that *STQ is real*. Moreover, the Standard Model is generalized and provides then insight into the nature and properties of DM particles. This can also be tested by applying these concepts to cosmology [11] and astrophysical observations.

We did this here in various ways. STQ predicts that DM particles interact by exchanging  $N_2$  bosons and that elastic scattering is predominant for the cosmic DM gas. The resulting *pressure* is proportional to the density of DM particles and increases thus when the DM gas is compressed by gravitational forces. This leads to the concept of *DM atmospheres* in hydrostatic equilibrium. It accounts very well for observed properties of DM halos for spiral galaxies. It appeared also that the mass of the central black hole is irrelevant. DM atmospheres could even contain only a small amount of baryonic matter, as has been observed.

The same concepts were applied to the DM atmosphere of the Sun and to explain the *stability* of the Oort cloud. DM atmospheres are also very important to prevent gravitational collapse of globular star clusters and cosmic filaments, where stars and galaxies remain separated from one another by being *embedded* in DM atmospheres. Moreover, there are *rotating DM rings* in the ecliptic plane of the Solar system. They explain the *Pioneer anomaly*. We proposed a mechanism that explains how planets sweep up all DM that is orbiting at the same distance from the Sun. This does usually protect them from gravitational effects of all DM rings in the ecliptic plane. It explains also why planets have their own DM disk. It is rotating in their equatorial plane and accounts for the *flyby anomaly*. Properties of this DM disk can also be studied by means of GPS satellites.

We provided already some information concerning the possible production and detection of DM particles [10]. We showed here that STQ allows also for DM-electron interactions. This explains why galactic DM could already be detected by the DAMA collaboration. We advanced also some reasons to reject not yet the possibility that the weak 3.5 keV *x-ray* signal might be produced by light DM particles. The global conclusion is that STQ and the resulting dark matter theory withstood the test of a detailed and varied confrontation with astrophysical observations. Reality is more astonishing than we thought.

## References

- [1] Zwicky, F. (1933) *Helvetica Physica Acta*, **6**, 110-127.  
<http://adsabs.harvard.edu/abs/1933AcHPh...6..110Z>
- [2] Rubin, V and Ford, W.K. (1970) *The Astrophysical Journal*, **159**, 379-403.  
<http://adsabs.harvard.edu/full/1970ApJ...159..379R>

- [3] Rubin, V., *et al.* (1976) *The Astronomical Journal*, **81**, 719-737.  
<http://adsabs.harvard.edu/full/1976AJ.....81..719R>  
<https://doi.org/10.1086/111943>
- [4] Rubin, V., *et al.* (1980) *The Astrophysical Journal*, **238**, 471-487.  
<http://adsabs.harvard.edu/full/1980ApJ...238..471R7>
- [5] Bosma, A. (1981) *The Astronomical Journal*, **86**, 1791-1824.  
<http://adsabs.harvard.edu/full/1981AJ.....86.1791B>  
<https://doi.org/10.1086/113062>
- [6] Bosma, A. (1981) *The Astronomical Journal*, **86**, 1825-1846.  
<http://adsabs.harvard.edu/full/1981AJ.....86.1825B>
- [7] Brownstein, J.R. and Moffat, J.W. (2005) *The Astrophysical Journal*, (2006) **636**, 721-741. <https://arxiv.org/abs/astro-ph/0506370>
- [8] McGaugh, S.S., *et al.* (2016) *Physical Review Letters*, **117**, 201101, 1-5.  
<https://arxiv.org/pdf/1609.05917.pdf>
- [9] Science News (2016) In Rotating Galaxies, Distribution of Normal Matter Precisely Determines Gravitational Acceleration.  
<https://www.sciencedaily.com/releases/2016/09/160921085052.htm>
- [10] Meessen, A. (2017) *Journal of Modern Physics*, **8**, 35-56.  
<http://dx.doi.org/10.4236/jmp.2017.81004>
- [11] Meessen, A. (2017) *Journal of Modern Physics*, **8**, 251-267.  
<https://doi.org/10.4236/jmp.2017.82017>
- [12] Navarro, J.F. Frenk, C.S. and White, S.D. (1996) *The Astrophysical Journal*, **462**, 563-575. <http://arxiv.org/abs/astro-ph/9508025>  
<https://doi.org/10.1086/177173>
- [13] Burkert, A. and Silk, J. (1999) On the Structure and Nature of DM Halos.  
<https://cds.cern.ch/record/384623/files/9904159.pdf>
- [14] Einasto, J. (1965) Kinematics and Dynamics of Stellar Systems, Trudy Inst. Astrofiz. Alma-Ata 5, 87.
- [15] Merritt, D., *et al.* (2006) *The Astronomical Journal*, **132**, 2685-2700.  
<http://arxiv.org/pdf/astro-ph/0509417v2.pdf>  
<https://doi.org/10.1086/508988>
- [16] Di Cintio, A., *et al.* (2010) *Monthly Notices of the Royal Astronomical Society*, **000**, 1-11, (2013). <http://arxiv.org/pdf/1204.0515.pdf>
- [17] Spergel, D.N. and Steinhardt, P.J. (2000) Observational Evidence for Self-Interacting Cold Dark Matter. <https://arxiv.org/pdf/astro-ph/9909386v2.pdf>
- [18] Kruezi, L. (2015) The Case for Complex Dark Matter. *Interview of James Bullock*, Quanta Magazine.  
<https://www.quantamagazine.org/20150820-the-case-for-complex-dark-matter/>
- [19] Erben, T., *et al.* (2000) *A&A*, **355**, 23. <https://arxiv.org/abs/astro-ph/9907134>
- [20] Capelato, H.V., *et al.* (2008) *A&A*, **492**, 345. <https://arxiv.org/abs/0809.2418>
- [21] van Dokkum, P., *et al.* (2016) *The Astrophysical Journal Letters*, **828**, 1.  
<https://arxiv.org/abs/1606.06291>
- [22] Feltzman, R. (2016) A New Class of Galaxy Has Been Discovered, One Made Almost Entirely of Dark Matter. The Washington Post, 25 August 2016.
- [23] Tully, R.B. and Fischer, J.R. (1977) *Astronomy & Astrophysics*, **54**, 661-673.  
<http://www.wikiwand.com/sv/Tully-Fisher-relationen>
- [24] Read, J.I. (2014) The Local DM Density. JPhysG-100038.R1.

- <https://arxiv.org/abs/1404.1938>
- [25] Pitjec, N.P. and Pitjeva, E.V. (2013) *Astron. Zhurnal or Astronomy Letters*, **39**, 141-149. <https://arxiv.org/abs/1306.5534>
- [26] Jeans, J.H. (1913) *MNRAS*, **74**, 109-112.  
<http://adsabs.harvard.edu/full/1913MNRAS..74..109J>  
<https://doi.org/10.1093/mnras/74.2.109>
- [27] Taylor, M.A., *et al.* (2015) *The Astrophysical Journal*, **805**, 1-20.  
<http://arxiv.org/pdf/1503.04198.pdf>
- [28] Caimmi, R. (2009) *Serbian Astronomical Journal*, **179**, 31-47.  
<http://arxiv.org/pdf/0909.3056.pdf>
- [29] Cappellari, M., *et al.* (2015) *The Astrophysical Journal Letters*, **804**, L21.  
<http://arxiv.org/pdf/1504.00075.pdf>
- [30] Harvey, D., *et al.* (2015) *Science*, **347**, 1462-1465.  
<https://arxiv.org/pdf/1503.07675.pdf>  
<https://doi.org/10.1126/science.1261381>
- [31] National Radio Astronomy Observatory (2014) Birth of Planets Revealed in Astonishing Detail in ALMA's Best Image.  
<https://public.nrao.edu/news/pressreleases/planet-formation-alma>
- [32] Bovaird, T. and Lineweaver, C.H. (2013) *MNRAS*, **435**, 1126-1138.  
<http://arxiv.org/pdf/1304.3341v4.pdf>
- [33] Nieto, M.M. (2005) *Physical Review D*, **72**, Article ID: 083004.  
<http://arxiv.org/abs/astro-ph/0506281>  
<https://doi.org/10.1103/PhysRevD.72.083004>
- [34] Anderson, J.D., *et al.* (1998) *Physical Review Letters*, **81**, 2858-2861.  
<http://arxiv.org/abs/gr-qc/9808081>  
<https://doi.org/10.1103/PhysRevLett.81.2858>
- [35] Turyshev, S.G. and Toth, V.T. (2010) *Living Reviews in Relativity*, **13**, 1-173.  
<http://arxiv.org/pdf/1001.3686>  
<https://doi.org/10.12942/lrr-2010-4>
- [36] Katz, J.I. (1998) *Physical Review Letters*, **83**, 1892.  
<http://arxiv.org/pdf/gr-qc/9809070v3.pdf>  
<https://doi.org/10.1103/PhysRevLett.83.1892>
- [37] Anderson, J.D., *et al.* (1999) *Physical Review Letters*, **83**, 1893.  
<http://arxiv.org/pdf/gr-qc/9906112v1.pdf>  
<https://doi.org/10.1103/PhysRevLett.83.1893>
- [38] Bertolami, O., *et al.* (2008) *Space Science Reviews*, **151**, 75-91 (2010).  
<http://arxiv.org/pdf/0809.2633.pdf>
- [39] Francisco, F., *et al.* (2012) *Physics Letters B*, **711**, 337-346.  
<http://arxiv.org/abs/1103.5222>  
<https://doi.org/10.1016/j.physletb.2012.04.034>
- [40] Rievers, B. (2012) High Precision Modeling of Thermal Perturbations with Applications to Pioneer 10 and Rosetta, Dissert. 1-169.  
<http://elib.suub.uni-bremen.de/edocs/00102500-1.pdf>
- [41] Turyshev, S.G., *et al.* (2012) *Physical Review Letters*, **108**, Article ID: 241101.  
<http://arxiv.org/abs/1204.2507>  
<https://doi.org/10.1103/PhysRevLett.108.241101>
- [42] Modenini, D. and Tortora, P. (2014) *Physical Review D*, **90**, Article ID: 022004.  
<http://arxiv.org/pdf/1311.4978.pdf>

- <https://doi.org/10.1103/PhysRevD.90.022004>
- [43] Turyshev, S.G., *et al.* (2006) *International Journal of Modern Physics D*, **15**, 56.  
<http://arxiv.org/abs/gr-qc/0512121>  
<https://doi.org/10.1142/S0218271806008218>
- [44] Moore, G.S.M. and Moore, R.E.M. (2013) *Astrophysics and Space Science*, **347**, 235-247. <http://link.springer.com/article/10.1007/s10509-013-1514-2>
- [45] Iorio, L. and Gioudice, G. (2006) *New Astronomy*, **11**, 600-607.  
<http://arxiv.org/abs/gr-qc/0601055>  
<https://doi.org/10.1016/j.newast.2006.04.001>
- [46] Tangen, K. (2007) *Physical Review D*, **76**, Article ID: 042005.  
<http://arxiv.org/abs/gr-qc/0602089>  
<https://doi.org/10.1103/PhysRevD.76.042005>
- [47] Wilkins, A. (2010) NASA.  
<http://io9.gizmodo.com/5584149/see-the-amazing-moon-inside-saturns-rings>
- [48] Anderson J.M. and Nieto, M.M. (2009) *Proceedings of the IAU Symposium*, **261**.  
<http://arxiv.org/abs/0907.2469>
- [49] Lämmerzahl, C., Preus, O. and Dittus, H. (2007) *Astrophysics and Space Science Library*, **349**, 75-101. <http://www.uv.es/jfgf/Pioneer/0604052.pdf>
- [50] Iorio, L. (2014) *International Journal of Modern Physics D*, **24**, 1530015, 1-35.  
<http://arxiv.org/abs/1412.7673>
- [51] Krasinsky, G.A. and Brumberg, V.A. (2004) *Celestial Mechanics and Dynamical Astronomy*, **90**, 267-288. [http://www.aldebaran.cz/bulletin/2009\\_24/GAKVAB.pdf](http://www.aldebaran.cz/bulletin/2009_24/GAKVAB.pdf)
- [52] Anderson, J.D., *et al.* (2008) *PRL*, **100**, Article ID: 091102, 1-4.  
[http://virgo.lal.in2p3.fr/NPAC/relative\\_fichiers/anderson\\_2.pdf](http://virgo.lal.in2p3.fr/NPAC/relative_fichiers/anderson_2.pdf)
- [53] Jouannic, B., *et al.* (2015) The Flyby Anomaly: An Investigation into Potential Causes. *Proc. 25th Internat. Symp. Space Flight Dynamics*, 1-17.  
[http://issfd.org/2015/files/downloads/papers/153\\_Jouannic.pdf](http://issfd.org/2015/files/downloads/papers/153_Jouannic.pdf)
- [54] NASA, Solar System Dynamics, Horizons Webb-Interface.  
<http://ssd.jpl.nasa.gov/horizons.cgi>
- [55] Adler, S. (2009) Is There Dark Matter in Orbit around the Earth? Institute Adv. Studies. <https://www.ias.edu/ideas/2009/adler-dark-matter>
- [56] Harris, R. (2013) Searching for Dark Matter using Navigation Satellites, American Geophysical Union, Fall Meeting.  
<http://adsabs.harvard.edu/abs/2013AGUFM.G21A0752H>
- [57] [www.newscientist.com/article/mg22129503-100-gps-satellites-suggest-earth-is-heavy-with-dark-matter/](http://www.newscientist.com/article/mg22129503-100-gps-satellites-suggest-earth-is-heavy-with-dark-matter/)
- [58] M. Francis.  
<http://galileospendulum.org/2014/01/02/no-dark-matter-is-not-messing-up-gps-measurements/>
- [59] LUX (Large Underground Xenon) Collaboration (2016) Results from a Search for Dark Matter in the Complete LUX Exposure. <http://arxiv.org/pdf/1608.07648.pdf>
- [60] Drukier, A., Freese, K. and Spergel, N. (1986) *Physical Review D*, **33**, 3495-3508.  
<http://kicp.uchicago.edu/~collar/drukier.pdf>  
<https://doi.org/10.1103/PhysRevD.33.3495>
- [61] Barnabei, R., *et al.* (2003) *La Rivista del Nuovo Cimento*, **26**, 1-73.  
<https://arxiv.org/abs/astro-ph/0307403>
- [62] Barnabei, R., *et al.* (2014) *Advances in High Energy Physics*, **2014**, Article ID: 605659, 1-10. <https://www.hindawi.com/journals/ahep/2014/605659/>

- [63] Barnabei, R., *et al.* (2008) *Physical Review D*, **77**, Article ID: 023506, 1-15.  
<https://arxiv.org/abs/0712.0562>  
<https://doi.org/10.1103/physrevd.77.023506>
- [64] Roberts, B.M., *et al.* (2016) *Physical Review D*, **93**, Article ID: 115037, 1-23.  
<https://arxiv.org/abs/1604.04559>  
<https://doi.org/10.1103/physrevd.93.115037>
- [65] Alkali Halides. <http://www.ucl.ac.uk/~ucapahh/research/crystal/homepage.htm>
- [66] Aalseth, C.E., *et al.* (2014) Search for An Annual Modulation in Three Years of Co-GeNT Dark Matter Detector Data. <https://arxiv.org/pdf/1401.3295v1.pdf>
- [67] Bulbul, E., *et al.* (2014) *The Astrophysical Journal*, **789**, 23 p.  
<https://arxiv.org/abs/1402.2301>
- [68] Boyarsky, A., *et al.* (2014) *Physical Review Letters*, **113**, Article ID: 251301.  
<http://arxiv.org/abs/1402.4119>  
<https://doi.org/10.1103/PhysRevLett.113.251301>
- [69] Boyarsky, A., *et al.* (2015) *Physical Review Letters*, **115**, Article ID: 161301.  
<https://arxiv.org/abs/1408.2503>  
<https://doi.org/10.1103/PhysRevLett.115.161301>
- [70] Carlson, E., Jeltema, T. and Profumo, S. (2015) *Journal of Cosmology and Astroparticle Physics*, **2015**, 1-27. <https://arxiv.org/abs/1411.1758>  
<https://doi.org/10.1088/1475-7516/2015/02/009>
- [71] Shah, C., *et al.* (2016) Laboratory Measurements Compellingly Support Charge-Exchange Mechanism for the “Dark Matter” ~3.5 keV X-Ray Line.  
<https://arxiv.org/abs/1608.04751>



**Submit or recommend next manuscript to SCIRP and we will provide best service for you:**

Accepting pre-submission inquiries through Email, Facebook, LinkedIn, Twitter, etc.

A wide selection of journals (inclusive of 9 subjects, more than 200 journals)

Providing 24-hour high-quality service

User-friendly online submission system

Fair and swift peer-review system

Efficient typesetting and proofreading procedure

Display of the result of downloads and visits, as well as the number of cited articles

Maximum dissemination of your research work

Submit your manuscript at: <http://papersubmission.scirp.org/>

Or contact [jmp@scirp.org](mailto:jmp@scirp.org)